NATIONAAL INSTITUUT VOOR KERNFYSICA EN HOGE-ENERGIEFYSICA

Afdelingsrapport
Theorie-82-1

J.H. KOCH

PHOTONUCLEAR REACTIONS AT INTERMEDIATE ENERGY

Invited talk at the Workshop on
"Electron rings for nuclear structure research"
Lund, October 5-7, 1982

AFDELINGS RAPPORT

THEORIE 82-1

NIKHEF SECTIE-K POSTBUS 4395, 1009 AJ AMSTERDAM

PHOTONUCLEAR REACTIONS AT INTERMEDIATE ENERGY

JUSTUS H. KOCH

National Institute for Nuclear
and High Energy Physics
Amsterdam
The Netherlands

Invited talk at the workshop on "Electron Rings for Nuclear Structure Research", Lund, Oct. 5-7, 1982

NIKHEF-K
Preprint P-107

PHOTONUCLEAR REACTIONS AT INTERMEDIATE ENERGIES

JUSTUS H. KOCH

NATIONAL INSTITUTE FOR NUCLEAR AND HIGH ENERGY PHYSICS, AMSTERDAM, THE NETHERLANDS

I. INTRODUCTION

The dominant feature of pion-and photon-nucleon interactions at intermediate energies is the excitation of the Δ resonance. Therefore, one can use pion- and photon-induced nuclear reactions to study the dynamics of Δ propagation in a nucleus. While a large number of experiments has been carried out with pions, the data base for photonuclear reactions for photon energies between 200 and 400 MeV is rather small. However, major experimental programs are now underway or planned for the new electron scattering facilities.

Fig. 1 shows the total photoabsorption cross section for a proton [1]. It clearly shows the Δ peak. If we subtract out the contribution from the $M_{1+}(3/2)$ multipole (dashed line), the remaining background is nearly energy independent. The peak cross section is about .5 mb, compared to 200 mb for π^+p scattering. This large cross section for pions implies that pion-nucleus scattering is mainly taking place in the nuclear surface. On the other hand, due to their much weaker interaction photons can reach the entire nuclear volume. One would therefore expect that the total nuclear photoabsorption cross section, $\sigma_{\gamma A}$, is simply given by $\sigma_{\gamma A} = A\sigma_{\gamma N}$, the incoherent sum of the nucleon cross sections. Fig. 2 shows the total photoabsorption data for ^{9}Be from Mainz [2] and Bonn [3]. Compared to the incoherent sum $A\sigma_{\gamma N}$ (solid line), the experimental cross section shows a substantial damping in the Δ region. A meaningful theoretical description must take into account the modification of the Δ propagation in the nuclear medium due to effects such as Fermi motion, nucleon binding or pion absorption. The Δ-hole formalism, which has been applied to π-nucleus scattering [4,5,6] offers a framework to consistently include these effects into the description of photonuclear reactions [7-12]. This approach is indicated in Fig. 3, where the same Δ-hole Green's function, $G_{\Delta h}$, is used in π-nucleus elastic scattering, nuclear Compton scattering and coherent π^0 photoproduction. Through the optical theorem, the forward Compton amplitude yields the total photoabsorption cross section. The

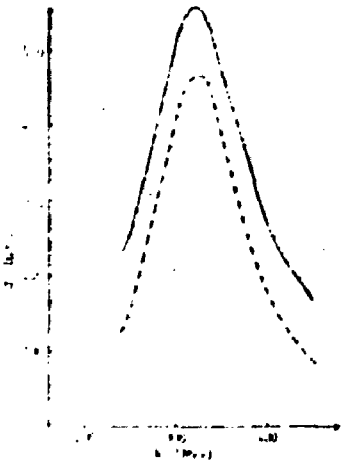

Fig. 1

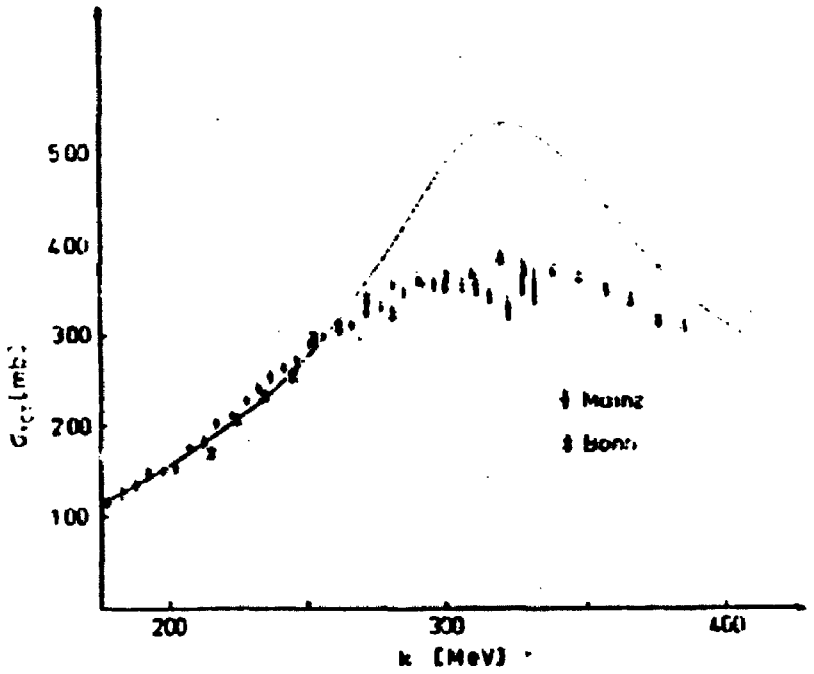

Fig. 2

reactions in Fig.3 correspond to different matrix elements of $G_{\Delta h}$. Pion-nucleus elastic scattering involves only Δ-h states with unnatural parity, while the photon also excites the natural parity Δ-h states. Another difference is that the $\pi N \to \Delta$ coupling is longitudinal, while the $\gamma N \to \Delta$ coupling is transverse. Photonuclear reactions therefore provide an important independent tool for studying the dynamics of Δ propagation in the nuclear medium.

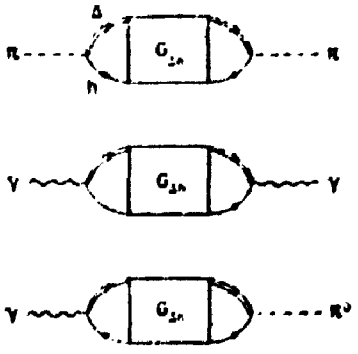

Fig. 3

In Section II we will first comment on photoabsorption on a single nucleon. A review of the Δ-h Greens function and of the photonuclear amplitude is given in Section III. Results for photoabsorption on ^{4}He are shown in Section IV and compared with the data. Coherent π^0 photoproduction is discussed in Section V and calculations for ^{12}C are compared to recent measurements. Section VI contains a short summary. The results used in this paper are taken from work done in collaboration with E.J. Moniz (MIT) and N. Ohtsuka (NIKHEF-K).

II. THE PHOTON-NUCLEON AMPLITUDE

To calculate the nuclear photoabsorption cross section, we first need a model for Compton scattering from a nucleon. We will assume that this proceeds through intermediate pion production in the πN s-wave and $M_{1+}(3/2)$ channels. The contribution from the Δ has the form

$$T_{\Delta}^{\gamma\gamma} = F^{+}_{\gamma N\Delta} \frac{1}{D(E)} F_{\gamma N\Delta}, \qquad (1)$$

where the transverse $\gamma N\Delta$ coupling is given by

$$F_{\gamma N\Delta} = \frac{G_{\gamma N\Delta}}{M_\Delta} \vec{\varepsilon} \cdot \vec{k} \times \vec{S}^+ T_3^1 \qquad (2)$$

and $D(E)^{-1}$ is the free Δ propagator, $D(E) = E - E_R + i\Gamma(E)/2 = \frac{\Gamma(E)}{2}(i - \mathrm{ctg}\delta_{33}(E))$. δ_{33} is the πN scattering phaseshift.
The optical theorem relates the imaginary part of the forward scattering amplitude of $T_\Delta^{\gamma\pi}$ to pion photoproduction. In the Δ-model, the $\gamma N \to \pi N$ amplitude is given by

$$T_\Delta^{\gamma\pi} = F_{\pi N\Delta}^+ \frac{1}{D(E)} F_{\gamma N\Delta}. \qquad (3)$$

Since $F_{\pi N\Delta}$ and $D(E)$ can be obtained from pion scattering, the only parameter remaining in Eqs. 1 and 3 is the coupling strength $G_{\gamma N\Delta}$. To reproduce the experimental $M_{1+}(3/2)$ multipole [1] at resonance, where $\mathrm{Re}M_{1+}(3/2) = 0$, we obtain $G_{\gamma N\Delta}/M_\Delta = .167$ f. However, this does not describe the observed energy dependence of the $M_{1+}(3/2)$ multipole very well. For a good fit, one has to include also non-resonant π production in the (3,3) channel [13]. If we add such a term, we must make sure that the total amplitude keeps the πN scattering phase δ_{33}. This is required by "Watson's final state theorem" [14]. When adding a non-resonant Born term $T_B(E)$, we can satisfy this requirement by letting the pion produced via T_B rescatter through the Δ. This is indicated in Fig. 4a. where T_B is represented by a black dot. Since we are interested in the Δ, we regroup the terms according to Fig. 4b. and work with T_B and a Δ-term with an effective or "dressed" $\gamma N\Delta$-vertex, $\tilde{F}_{\gamma N\Delta}$, indicated by the shaded circle. Formally, the effective vertex is defined by

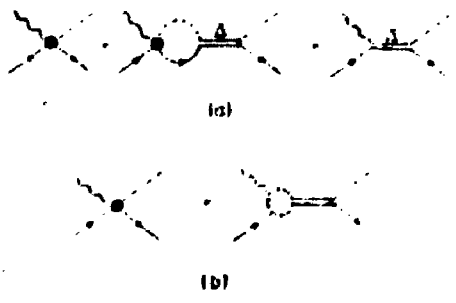

Fig. 4

$$T_{3,3}^{\gamma\pi}(E) = (1 + T_\Delta^{\pi N}(E) G^{\pi N}(E)) T_B^{\gamma\pi}(E) + T_\Delta^{\gamma\pi}(E)$$
$$\equiv T_B^{\gamma\pi}(E) + F_{\pi N\Delta}^+ \frac{1}{D(E)} \tilde{F}_{\gamma N\Delta}(E). \qquad (4)$$

Through the intermediate πN rescattering in $\tilde{F}_{\gamma N\Delta}$, this effective vertex is energy dependent and complex. This partitioning of the measured multipole into a resonant and non-resonant part is clearly model dependent. Rather than calculating this effective vertex from a model, the standard approach has been to simply parametrize [11,13,15]

$$\tilde{F}_{\gamma N\Delta}(E) = e^{i\phi(E)} F_{\gamma N\Delta}, \qquad (5)$$

where $\phi(E)$ is a smooth function of energy. With this parametrization we obtain for the full 3,3 amplitude, Eq. 4,

$$T^{\gamma,\pi}_{3,3} = F^{+}_{\pi N\Delta} F_{\gamma N\Delta}\left(-\frac{\sin\phi}{\Gamma(E)/2} + \frac{e^{i\phi}}{D(E)}\right), \qquad (6)$$

which satisfies Watson's theorem. Similarly the full 3,3-Compton amplitude becomes

$$T^{\gamma,\gamma}_{3,3} = F^{+}_{\gamma N\Delta} \frac{1}{D(E)} F_{\gamma N\Delta} e^{2i\phi(E)} + T^{+}_{B} G^{\pi N}(E) T_{B}. \qquad (7)$$

Finally, to complete our description of photoabsorption, we also have to include other intermediate πN-channels. This contribution is mainly due to intermediate s-wave charged pion production. For the applications below, we simply use an amplitude of the Kroll-Ruderman form,

$$T^{\gamma\pi^{\pm}}_{s} \sim \vec{\sigma}.\vec{\epsilon}\; h(E),$$

where h(E) has been fitted to the data [12]. The model outlined above reproduces the total γN cross section very well for photon laboratory energies between 200 - 400 MeV. However, the fit in individual charge channels is poorer and we will use a refined model when discussing a specific reaction such as (γ,π^0) in Section V.

III. THE NUCLEAR PHOTOABSORPTION AMPLITUDE

We first discuss photoabsorption proceeding through Δ-h excitation only. The nuclear amplitude is

$$\langle\vec{k}';0|H^{\gamma\gamma}_{\Delta}|\vec{k};0\rangle = \langle\vec{k}';0|F^{+}_{\gamma N\Delta} G_{\Delta h}(E)\, F_{\gamma N\Delta} e^{2i\phi(E)}|\vec{k};0\rangle \qquad (8)$$

The many-body Greens function $G_{\Delta h}$ is given by [4,7,11]

$$G^{-1}_{\Delta h} = D(E - H_{\Delta}) - \delta W - W_{\pi} - V_{sp} \qquad (9)$$

$$H_{\Delta} = T_{\Delta} + V_{\Delta} + H_{A-1}. \qquad (10)$$

The first part of the Greens function is the free Breit-Wigner denominator, D(E), evaluated at $E - H_{\Delta}$, the internal energy available to the Δ. H_{Δ}, Eq. 10, includes the kinetic energy T_{Δ}, an average binding potential, V_{Δ}, and the hole energy H_{A-1}. The phasespace for $\Delta \to \pi N$ is restricted inside the nucleus. This is taken into account by the Pauli blocking term, δW, which reduces the free width and produces a repulsive shift of the resonance energy. W_{π} in Eq. 9 describes intermediate pion propagation with the target in the ground state, Fig. 5a. In elastic π-nucleus scattering, this term yields the very large elastic width due to coherent multiple scattering [9]. In the photoreactions considered here, it accounts for coherent π^0 photoproduction. The terms described so far can be evaluated microscopically in the Δ-h basis. As is known from pion scattering, it is important to take into account that the Δ-h states can couple to more complicated channels. In contrast to the other terms in Eq. 9 this effect is treated

phenomenologically through a complex spreading potential

$$V_{sp}(r) = V_C \frac{\rho(r)}{\rho(0)} + V_{LS} \, p r^2 p - p r^2 \, 2 l_\Delta \cdot t_\Delta \qquad (11)$$

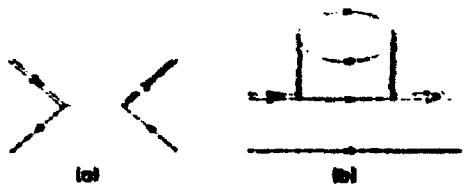

Fig. 5

The complex parameters, V_C and V_{LS}, have been obtained from fits to elastic pion-nucleon scattering and are nearly energy independent [16]. For example, for ^{4}He we have $\mathrm{Im}\, V_C \gtrsim -35$ MeV. It has been shown that this rather sizable spreading potential mainly describes the coupling to the pion absorption channel [4,16]. An example of this is given in Fig. 5b.

To obtain the total photoabsorption cross section, we use the optical theorem for the nuclear Compton amplitude, Eq. 8,

$$\sigma_\Delta^T = -\frac{1}{k} \mathrm{Im}\, M_\Delta^{\gamma\gamma}(\vec{k},\vec{k}) \frac{M_T}{k + M_T + \frac{k^2}{2M_T}} . \qquad (12)$$

In addition to predicting the total cross section, we can also use our model to partition σ^T into the major reaction channels [11,12]. The contributions to $\mathrm{Im}\, M_\Delta^{\gamma\gamma}$ are shown schematically in Fig. 6, where a wavy line indicates the on-shell part of a propagator. As shown in Fig. 6a, $\mathrm{Im}\, M_\Delta^{\gamma\gamma}$ has contributions from $\mathrm{Im}\, G_{\Delta h}$ and from the on shell part of the πN loop in $\tilde{P}_{\gamma N\Delta}$, which corresponds to quasifree πN photoproduction. The partitioning of $\mathrm{Im}\, G_{\Delta h}$ is shown in Fig. 6b: the first diagram corresponds to quasifree knockout, due to the imaginary part of $D(E-H_\Delta) - \delta W$, i.e. proceeding through the Pauli blocked isobar. The next contribution is due to $\mathrm{Im}\, W_\pi$ and yields the coherent π^0 photoproduction partial cross section. Finally, the last diagram indicates contributions from $\mathrm{Im}\, V_{sp}$, which accounts for the partial cross section into the π absorption channel. In addition to the isobar contribution, we have to take into account the 3,3 background amplitude T_B, Eq. 4, which leads to a πph state. We include

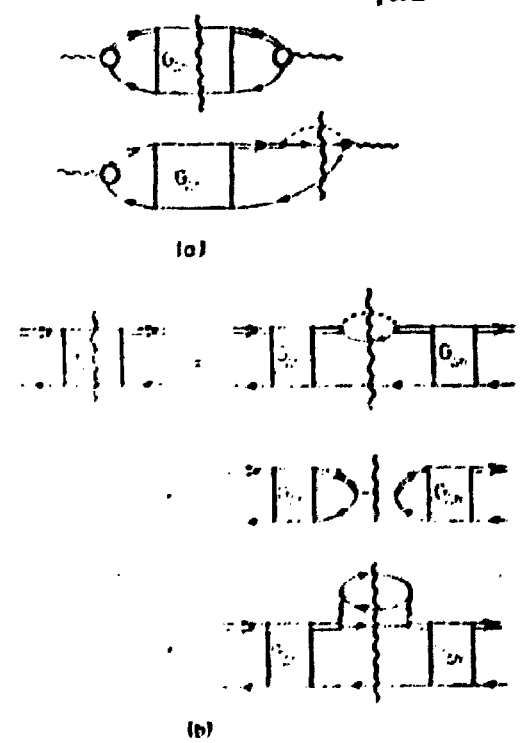

Fig. 6

this term in impulse approximation. In the unnatural parity partial waves, this term can also lead to coherent π^0 photoproduction. As shown in Fig. 7, the π^0 can then excite a Δh state, which can be considered as a density dependent $\gamma \to \Delta h$ vertex correction. We include this effect in our calculations below. Finally, we must also include the background term due to s-wave pion production. This is done in impulse approximation by using a local Fermi gas calculation.

Fig. 7

IV. PHOTOABSORPTION ON ^{4}He

Fig. 8 shows the isobar part σ_Δ^T, Eq. 12, of the total photoabsorption cross section for ^{4}He and its partitioning. The largest contribution comes from quasifree π production (QF). The quasifree and the much flatter absorption cross section both peak near the resonance energy of the free Δ. The coherent π^0 cross section peaks at a lower energy, because it depends on the nuclear ground state formfactor which drops rapidly with increasing momentum transfer. For heavier nuclei, this π^0 partial cross section is less important.

In calculating the photoabsorption cross section, many body effects enter in two ways: V_{sp}, for example, enters directly by contributing an absorption partial cross section to the nuclear cross section. But it also enters in the Δh propagators, $G_{\Delta h}$, and "shadows" all reaction channels (Fig. 6b). These two competing effects can be seen in Fig. 9, which shows the full calculation for the 3,3-channel photoabsorption cross section (solid line) and a calculation with V_{sp} omitted. At low energies, inclusion

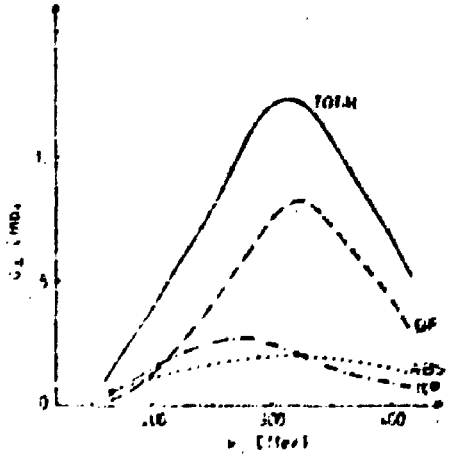

Fig. 8

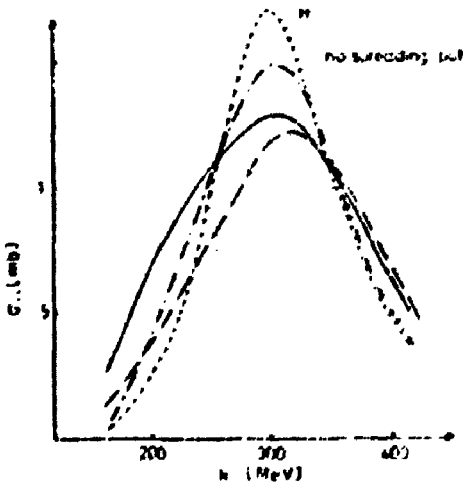

Fig. 9

of the absorption channel increases the cross section, but near resonance shadowing dominates and the cross section decreases. It is therefore not correct to separately add an absorption cross section in a perturbative way. Similar remarks apply to coherent π^0 production. The short dashed curve (H_Δ) shows a calculation which only keeps $D(E - H_\Delta)$ in the Δh-propagator, Eq. 10, which accounts for Δ propagation and binding effects. Inclusion of the many body terms, $\delta W + W_\pi + V_{sp}$, leads to a substantial broadening and depression of the peak cross section. The long dashed curve shows the results of omitting the coherent non-resonant π^0 production terms, Fig. 7, which has a large effect below resonance. (This effect is again much smaller for heavier nuclei.)

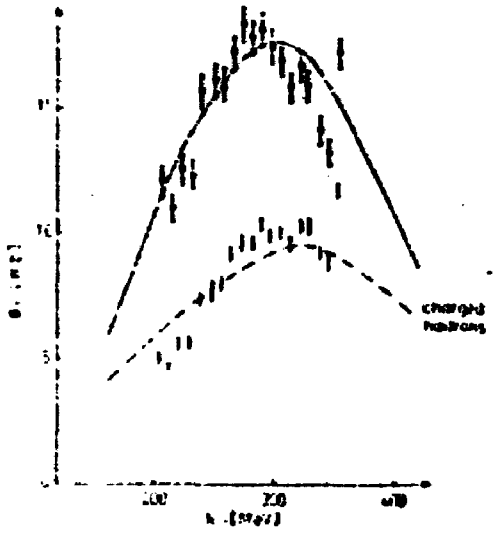

Fig. 10

Fig. 10 shows our results for the full photoabsorption cross section and the ^{4}He measurements of the Bonn group [17]. The total cross section data result from a sizeable extrapolation of the observed charged hadron yield (also shown) at five angles. Missed events due to energy cutoffs for charged hadrons and due to neutral events were estimated by comparing to a Monte Carlo cascade calculation at three energies for a ^{9}Be, ^{12}C, Ti and Pb target. By interpolation, these calculations were then used for other targets and different energies. The cross section for coherent π^0 calculation was calculated separately and added. (This ignores the shadowing effect discussed above.) We can use the decomposition of the cross section, Section III, to make a rough comparison with the measured charged hadron yield: we take the full s-wave contribution, the (3,3)-channel absorption cross section and one third of the (3,3) quasifree πN production cross section. We exclude coherent and quasifree π^0 production. Knocked out protons in the latter case are assumed to have energies below the experimental cutoff of 58 MeV. The agreement of this estimate with the data is quite good. The total cross section, which is much more reliably calculated, agrees fairly well with the extrapolated data below resonance. The calculated peak position is at a somewhat higher energy and above resonance too much cross section is predicted.

V. COHERENT π^0 PHOTOPRODUCTION

The Δ contribution tc the nuclear (γ,π^0)amplitude is

$$\langle \vec{q};0|M_\Delta^{\gamma\pi^0}|k;0\rangle = \langle \vec{q};0|F^+_{\pi N\Delta}\, G_{\Delta h}\, \tilde{F}_{\gamma N\Delta}|k;0\rangle \qquad (13)$$

To this we have to add the coherent π^0 contribution from the non-resonant term T_B, in Eq. 4. This term, together with the medium correction to Eq. 13 which arises from the modified $\gamma \to \Delta h$ vertex in Fig. 7, corresponds to a DWIA treatment of the background production through T_B. Since we are also interested in the angular π^0 distribution at lower energy, we have to include multipoles other than the $M_{1-}(3/2)$. These multipoles are small and have little effect on the total $\gamma p \to \pi^0 p$ cross section, but change the angular distribution due to interference with the $M_{1+}(3/2)$ multipole. We take these multipoles from Ref. 1 and include them in a distorted wave impulse approximation.

In Fig. 11, the total coherent π^0 photoproduction cross section on ^{12}C is shown keeping the full production operator, i.e. the resonant multipole $M_{1+}(3/2)$ and all other multipoles. The long dashed curve is the impulse approximation and the solid curve the result of the full calculation. Comparison is made with the data of Arends *et al.* [18]. It must be stressed that the data include not only coherent π^0 photoproduction but also π^0 production accompanied by excitation of particle stable target states. The resulting overestimate of the coherent cross section will be most severe at the higher photon energies, where larger momentum transfers to the nucleus are involved. Our calculation agrees reasonably well with the data for $k_\gamma \lesssim 250$ MeV and falls significantly below for higher energy. The calculation with no spreading potential is also shown in the figure (dash-dot). Below 300 MeV, the $V_{sp} = 0$ result is larger than the upper bound provided by the Bonn data. Thus, a strong spreading potential is required. While our model is consistent with the data, obviously a clean separation of the coherent π^0 cross section is needed for a quantitative test. Finally, Fig. 11 also shows the contribution from non-resonant coherent π^0 production alone (short dashed curve) which represents an appreciable part of the cross section at the lower energies.

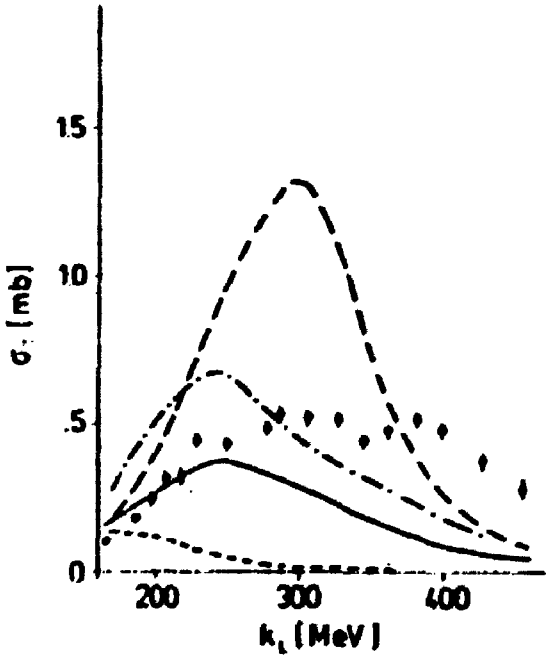

Fig. 11

In Fig. 12, we show two sets of data for $^{12}C(\gamma,\pi^0)^{12}C$ for photon energies $k_{lab} \gtrsim 240$ MeV. The old

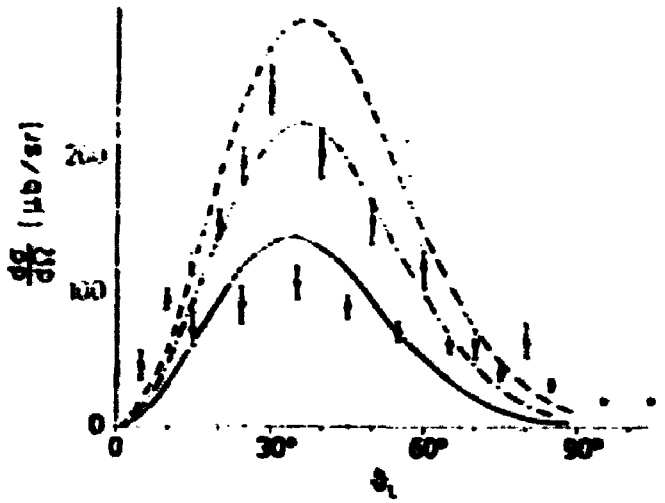

Fig. 12

Davidson data [19] (crosses) have long been the subject of controversy. Clearly the two data sets are in considerable disagreement. Our calculation with the complete $\gamma n \to \pi^0 n$ amplitude (solid curve) is about a factor of two smaller than the Davidson data. Note again that the full result is much smaller than either the impulse approximation result (dashed) or the result with no spreading potential (dash-dot). In comparing with the Bonn data [18] (dots), we see that the calculated cross section lies about 20% above the data at the peak and below the data at large angles. However, the Bonn data include photoproduction accompanied by excitation of particle stable target states, which will increase especially the large angle cross section. Furthermore, if one folds our predicted angular distribution with the experimental angular resolution for 100 MeV pions, the agreement with the data becomes better. Another problem in comparing the data to our calculation is the poor state of the low energy $\gamma p \to \pi^0 p$ data. Fig. 13 shows the differential cross section data available [20] for $k_L \approx 240$ MeV. The multipoles of Ref. 1, which we use (solid curve) fit the Bonn data [21] (filled circles), but not the measurements of Govorkov *et al.* [22] (diamonds), which extend to the forward region where the nuclear (γ,π^0) cross section peaks (see Fig. 12). The dashed curve, obtained from the $M_{1+}(3/2)$ multipole alone, fits the forward angle data better. A nuclear calculation with this multipole only would bring our prediction closer to the Davidson data. Clearly, new single nucleon data are needed to allow for a more reliable prediction of the nuclear coherent cross section at lower energies.

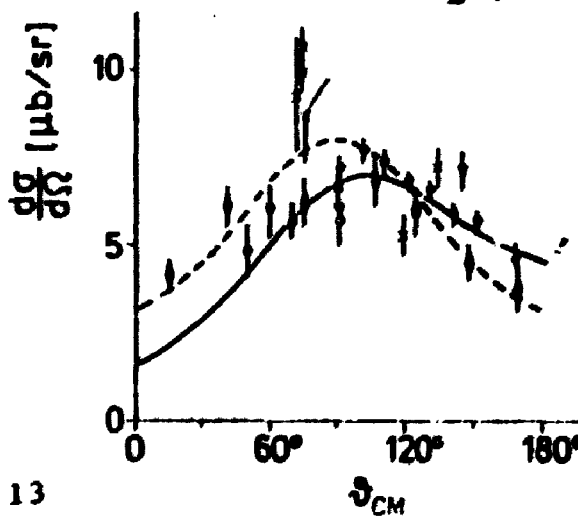

Fig. 13

Finally, as was shown in detail in Refs. 7 and 11, photoproduction calculated in the Δ-h approach consistently

includes many body effects in two ways: in the γN production step and in the distortion of the outgoing pion. The effects due to many body modifications of the pion production operator, which are not included in DWIA calculations, are very large for coherent π^0 photoproduction.

VI. SUMMARY

The Δ-hole approach provides a unified approach to study pion- and photon-induced nuclear reactions at intermediate energy. In this framework, we have seen that the many body modifications of Δ-h propagation, which were previously studied in pion scattering, also play an important role in photonuclear processes. Examples of this were shown for photoabsorption and coherent π^0 photoproduction. The detailed description of the Δ-h dynamics also allowed us to decompose the total photoabsorption cross section into the major reaction channels. This made it possible, for example, to compare directly to the measured charged hadron yield for photoabsorption on ^{4}He. Other applications, which were not discussed, are electron scattering (absorption of a virtual photon) and Compton scattering on nuclei. In addition to the data discussed here, there are only a few other experiments on photoabsorption and coherent π^0 photoproduction. Certainly, much more such experiments are needed, together with Compton and electron scattering at intermediate energies. Also, more single nucleon measurements are necessary to provide a reliable set of photopion multipoles, which are needed as input for nuclear calculations. Clearly, the theoretical description needs to be refined. For example, the use of a local spreading potential is certainly only an approximation and more complicated many body vertex corrections have to be included. Since the photon samples the nucleus in a different way than the pion, photonuclear reactions will be very important in advancing our understanding of Δ propagation in nuclei.

ACKNOWLEDGEMENT

This work is part of the research program of the National Institute for Nuclear and High Energy Physics (NIKHEF, section K), made possible by financial support from the Foundation for Fundamental Research on Matter (FOM) and the Netherlands Organisation for the Advancement of Pure Research (ZWO).

REFERENCES

1. F.A. Berends *et al.*, Nucl. Phys. B4 (1967) 54; Nucl. Phys. B84 (1975) 342
2. B. Ziegler in "Nuclear Physics with Electromagnetic Interactions", H. Arenhövel and D. Drechsel (eds) Springer Verlag (1979)
3. J. Arends *et al.*, Phys. Lett. 98B (1981) 423
4. M. Hirata, F. Lenz and K. Yazaki, Ann. Phys. (NY) 108 (1977) 116,
   M. Hirata, J.H. Koch, F. Lenz and E.J. Moniz, Ann. Phys. (NY) 120 (1978) 205

5. E. Oset and W. Weise, Nucl. Phys. A319 (1979) 477; Nucl. Phys. A329 (1979) 365
6. K. Klingenbeck, H. Dilling, M.G. Huber, Phys. Rev. Lett. 41 (1978) 387
7. J.H. Koch and E.J. Moniz, Phys. Rev. C20 (1979) 235
8. E.J. Moniz in "Nuclear Physics with Electromagnetic Interactions", (see Ref. 2).
9. W. Weise, Nucl. Phys. A358 (1981) 103; E. Oset and W. Weise, Nucl. Phys. A368 (1981) 375
10. K. Klingenbeck and M.G. Huber, Phys. Lett. 98B (1981) 15; J. Phys. G6 (1981) 375
11. J.H. Koch and E.J. Moniz, MIT preprint CTP 1018 (1982)
12. J.H. Koch in "The Study of Few Body systems with Electromagnetic Probes", Conf. Proceedings NIKHEF-K, Amsterdam (1981), p. 134; J.H. Koch, E.J. Moniz and N. Ohtsuka (in preparation)
13. M.G. Olsson, Nucl. Phys. B78 (1974) 55
14. M.L. Goldberger and K.M. Watson, "Collision Theory", John Wiley and Sons, New York (1967)
15. I. Blomquist and J.M. Laget, Nucl. Phys. A280 (1977) 405
16. Y. Horikawa, M. Thies and F. Lenz, Nucl. Phys. A345 (1980) 386
17. H. Rost, Dissertation, Universität Bonn (1980)
18. J. Arends *et al.*, Bonn preprint (1982)
20. D. Menze *et al.* "Physik Daten" (Karlsruhe) 7-1(1977)
21. H. Genzel *et al.*, Z. Phys. 268 (1974) 19
22. B. Govorkov *et al.*, J. Nucl. Phys. A280 (1977) 405